

PAPER • OPEN ACCESS

The Relationship between Morphology of Milling Surface and Its Corrosion Resistance for Nickel base Superalloy FGH97

To cite this article: Jinping Shi *et al* 2019 *IOP Conf. Ser.: Mater. Sci. Eng.* **484** 012028

View the [article online](#) for updates and enhancements.

The Relationship between Morphology of Milling Surface and Its Corrosion Resistance for Nickel base Superalloy FGH97

Jinping Shi^a, Peiquan Guo^{b,*}, Yang Qiao^c, Shouren Wang^d and Tonghui Liu^e

Department of Mechanical Engineering, University of Jinan, 336 Nanxinzhuanxi Road, Jinan, Shandong 250022, P.R. China.

Email: ^ame_shijp@ujn.edu.cn, ^boss_guopq@ujn.edu.cn, ^cme_qiaoy@ujn.edu.cn, ^dme_wangsr@ujn.edu.cn, ^etonghui_liu@163.com

Abstract. The relationship between morphology of milling surface and its corrosion resistance for nickel base superalloy FGH97 have been investigated based on the milling experiment corresponding to different cutting parameters. Motif area ratio parameter is proposed in order to visually characterize the surface morphology. Motif area ratio is defined as the ratio of the surface area that can meet the threshold condition to the machined surface. The morphology of the workpiece surface can be characterized by the amplitude parameter and Motif area ratio method. The relationship model between the milling parameters and the corrosion rate of the workpiece is established by taking surface morphology, residual stress and other surface characteristics as the intermediate variables. Experimental results show that the corrosion rate of the workpiece will be smaller and smaller as surface morphology improved. The higher the residual stress on the workpiece surface, the larger the corrosion rate of the workpiece will be.

1. Introduction

Powder superalloy is of excellent mechanical properties, thermal properties, thermal fatigue properties and high reliability. It is the preferred material for the key parts of modern aeroengine, such as turbine disc, guide vane, ship gas turbine, rocket engine and nuclear reactor. In the early 1970s, the P&WA Company of the United States first developed the IN100 powder superalloy, which is used in the turbine discs of F15 and F16 engines and other components. In order to improve the engine performance, GE successfully developed René88DT turbine disc by argon atomization (AA) and hot extrusion and isothermal forging in 1988. The turbine disc is widely used in civil and military aircraft. The outstanding characteristic of the second generation powder superalloys represented by René88DT is that the crack propagation rate is obviously reduced by 50% compared with the first generation superalloys, the maximum service temperature is up to 750 degrees Centigrade. [1, 2]. In the 1990s, the United States has developed the third generation powder superalloys, such as Alloy10, René104 and RR1000 [3, 4]. Superalloy FGH95, FGH96 and FGH97 alloys have been developed successively in the late 1970s in China. Superalloy FGH95 is characterized as high strength at working temperature of 650 degrees Centigrade. Superalloy FGH96 can be used at temperatures up to 700-750 degrees Centigrade. It is a key material for preparing high performance engine turbine disk. Superalloy FGH97 prepared by plasma rotating electrode pulverizing and hot isostatic pressing has the advantages of high tensile strength and high creep resistance, and its crack propagation rate is one order of magnitude lower than that of FGH95 or FGH96 [5-7]. In October 1971, an aircraft of VICHERS Company crashed due to corrosion-induced breakage of pressurized compartment. In August 1981, a B737-200 of Taiwan Far East Airlines crashed due to corrosion-induced large area perforation of fuselage skin. In August 1985, a Japanese B747 aircraft crashed due to corrosion-induced fatigue fracture of



pressurized compartment. In May 2005, a Boeing 747 of Taiwan crashed into the South China Sea due to corrosion-induced cracks in the tail wing. There are so many catastrophic accidents caused by corrosion that it is very important to study the effect of milling surface morphology on corrosion resistance of superalloy FGH97. A lot of research works about machining of nickel-based alloy have been done such as cutting forces and wear [8, 9], integrity of machined surface [10-13], machining induced residual stresses [14-16]. There is lack of research on its corrosion resistance.

2. FGH97 Milling Test

2.1. Properties of FGH97

The composition of FGH97 is shown in Table 1. The alloy elements dissolve a large number of solid solutions in Co and Ni, i.e. the strengthening phase γ' . In order to ensure good strengthening effect, the content of strengthening phase γ' in FGH97 is about 64% of the alloy mass fraction. Its tensile strength is 1510 MPa, yield strength is 1080 MPa and solid solution temperature is 1180-1190 degrees Centigrade. Therefore, the physical properties of FGH97 seriously restrict its machinability. Because of the special manufacturing process of materials, thermal-induced pores are formed in the material during the manufacturing process. When the tool cuts the induced pores, the tool will be impacted. The continuous impact has a great impact on the tool performance. Moreover, the existence of thermal-induced pores is not conducive to the heat dissipation during the cutting process. The thermal induced porosity also severely restricts the machinability of the material. So, FGH97 is very difficult to be machined.

Table 1. Composition of FGH97 (wt %).

C	Cr	Co	Al	Ti	W	Nb	Hf	B	Zr	Mg	Ce	Ni
0.04	9.0	15.5	4.9	1.8	5.5	2.6	0.3	≤ 0.015	≤ 0.015	≤ 0.02	≤ 0.01	bal

2.2. Test Condition

Milling experiments were conducted on a machining center YCM-V116B as shown in Figure 1. TiAlN-TiN coated carbide insert SECO made SEEX1204AFTN-MD18 is used to mill FGH97. Mill cutter consists of a cutter head R220.53-0100-15-5A and inserts mentioned above. Inserts are fixed on cutter head. Cutter's geometric parameters are rake angle of 10° , clearance angle of 12° , cutting edge angle of 30° , distortion angle of 3° , tool cutting edge inclination angle of -10° .



Figure 1. Machining center and cutter.

3. Morphology Characterization of Milling Surface

3.1. Amplitude Parameter Characterization Method

Under the condition of same feed per tooth and depth of cut, the influence of cutting speed on 3D surface topography parameters is shown in Figure 2. When the speed is in range of 30-70m/min, the value of kurtosis S_{ku} and partial slope S_{sk} is higher, however, the other parameter values are relatively small. This suggests that the surface morphology is better. When the cutting speed is 90m/min, the parameter values are generally higher, especially S_v and S_z , which shows that there are relatively large and deep valleys on the surface. This is because when the cutting speed is 90m/min, for machining of

nickel base powder metallurgy superalloy, it has been in range of high-speed cutting. In such case, cutting temperature and tool rotational speed are very high; the vibration of machine tool system is relatively large. For this reason, it eventually makes surface topography bad.

Under the condition of same cutting speed and depth of cut, the influence of feed per tooth on 3D surface topography parameters is shown in Figure 3. As shown in Figure 3, in addition to kurtosis S_{ku} and partial slope S_{sk} , with the increase of feed per tooth other amplitude parameters also subsequently increased. When the feed per tooth is 0.05mm/z, $S_{sk}<0$ and $S_{ku}>3$. This shows that there are relatively steep valleys which affect the quality of 3D surface topography. When the feed per tooth is 0.10mm/z, the value of each magnitude parameter is relatively small, in addition, the value of slope S_{sk} is close to zero and the kurtosis $S_{ku}<3$. This shows that the surface is smooth and no larger peaks and valleys exist. Therefore, when the feed per tooth is 0.10mm/z, the 3D surface topography of workpiece is the best.

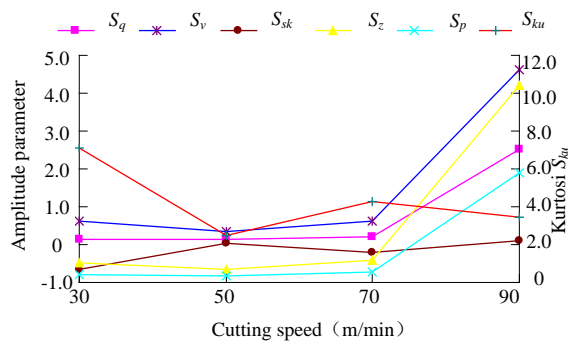


Figure 2. Influence of v on surface topography.

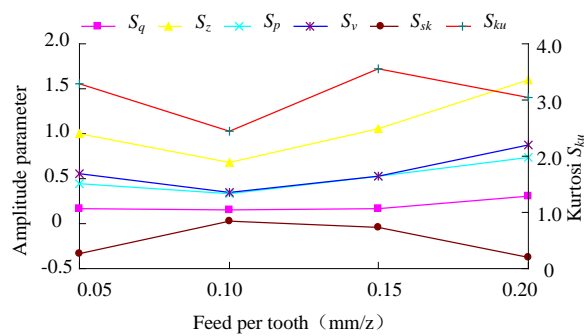


Figure 3. Influence of f_z on surface topography.

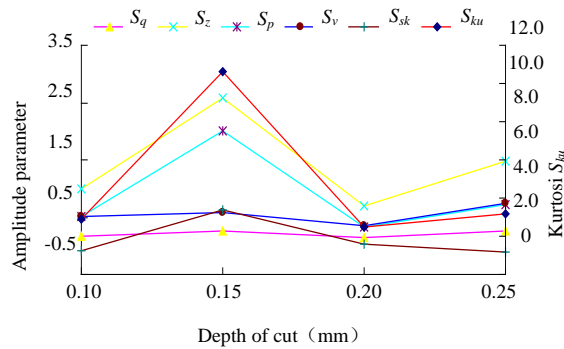
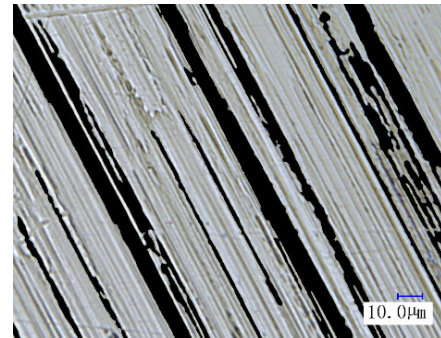
Under the condition of same cutting speed and feed per tooth, the influence of depth of cut on 3D surface topography parameters is shown in Figure 4. When the depth of cut is 0.15mm, after the completion of the cutting each amplitude parameters are relatively large, in addition, $S_{ku}>3$ and $S_{sk}>0$. This shows that there distribute relatively steep peaks on the surface, which affect the quality of the surface topography.

3.2. Motif Area Ratio Characterization Method

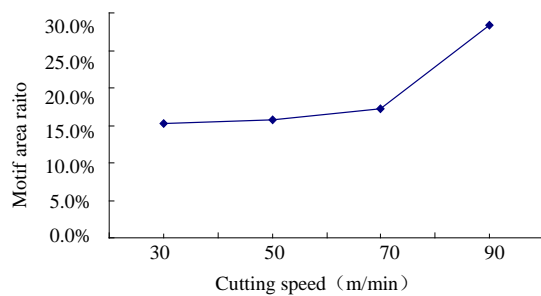
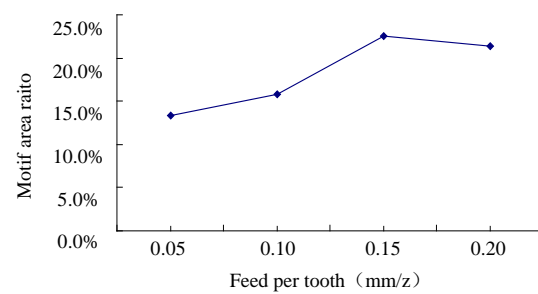
In order to be more intuitive to characterize the surface morphology of different milling parameters and evaluate the degree of corrosion, this paper defines Motif area ratio parameter. It is defined as the ratio of the surface area that can meet the threshold condition to the machined surface. The formula is shown as Equation (1). The selection of threshold need to consider the actual situation that does not affect the subsequent experimental results. As shown in Figure 5, the black area represents the Motif area that meet the threshold condition. In this experiment, the selection of threshold area does not affect the result of surface morphology on corrosion resistance of the workpiece.

$$P_s = \frac{\sum_{i=1}^n S_i}{S} \times 100\% \quad (1)$$

Where P_s is the Motif area ratio, S_i is the surface area that meets the threshold condition; S is the whole surface area.

**Figure 4.** Influence of a_p on surface topography.**Figure 5.** Motif area distribution.

With the increase of cutting speed, the Motif area ratio starts smoothly and then increases rapidly. From Figure 2 and Figure 6, we can find that the result of Motif area ratio method is close to the amplitude parameter characterization method. As shown in Figure 7, with the increase of feed per tooth, Motif area ratio increases gradually. In the process of cutting, with the increase of feed per tooth, cutting force and plastic deformation become larger. Therefore, the scallop height on workpiece increases so as to increase the Motif area ratio.

**Figure 6.** Relationship between cutting speed and Motif area ratio.**Figure 7.** Relationship between feeding per tooth and Motif area ratio.

It can be seen from Figure 8 that the influence of depth of cut on surface Motif area ratio is not obvious, but because of the Motif area ratio value itself is at a relatively high position, mean value at around 20%. Therefore, we can conclude that the depth of cut has a significant influence on Motif area ratio.

4. Relationship between Surface Morphology and Corrosion

4.1. Immersion Corrosion Test

Immersion corrosion test has been done in order to simulate marine environment. All surfaces of the specimen are painted except for machined surface in order to avoid corrode. The test time is 1200h and the experimental process reference JB/T 7901-1999 (metallic materials laboratory uniform immersion corrosion test method). Average corrosion rate can be used to evaluate test result as shown in Equation (2).

$$V_a = \frac{kW}{At\rho} \quad (2)$$

Where V_a is average corrosion rate, k is a constant, W is corrosion weight loss, A is sample surface area, t is test time, ρ is the density of the material.

4.2. Influence of Cutting Parameters on Corrosion

The surface roughness of the workpiece is extracted from the 3D surface topography information, and the variation law of the average corrosion rate and the surface roughness is drawn into curves as shown in Figure 9, 10 and 11. They respectively indicate the influence of cutting speed, feed of per tooth or depth of cut on corrosion.

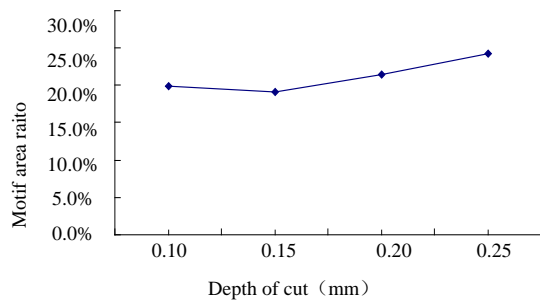


Figure 8. Relationship between depth of cut and Motif area ratio.

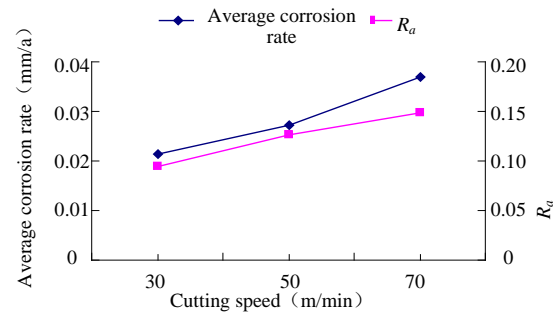


Figure 9. Influence of cutting speed on surface roughness and corrosion rate.

Compared to the average corrosion rate curve and the surface roughness curve can be found that the change tendency of both is basically the same, when the value of the surface roughness increases, the average corrosion rate becomes larger; when the value of surface roughness is small, the average corrosion rate is smaller. That is to say average corrosion rate of workpiece varies with the change of surface roughness. When the cutting speed is 90m/min, there occurs tool tipping, so in this paper we omit the corrosion result out of Figure 9.

When the feed per tooth is 0.05mm/z, from the figure can be found that the value of average corrosion rate reaches the maximum. However the surface roughness is very small, which is due to measurement error that led to this result. Thus, we omit this data point out of Figure 10. When the feed per tooth is in range of 0.10-0.20mm/z, average corrosion rate increases when surface roughness becomes larger as shown in Figure 10. As shown in Figure 11, it can be found that along with the change of axial cutting depth, change low of average corrosion rate is consistent with the change of surface roughness.

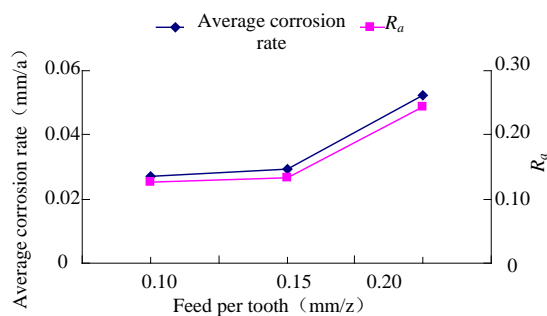


Figure 10. Influence of feeding per tooth on surface roughness and corrosion rate.

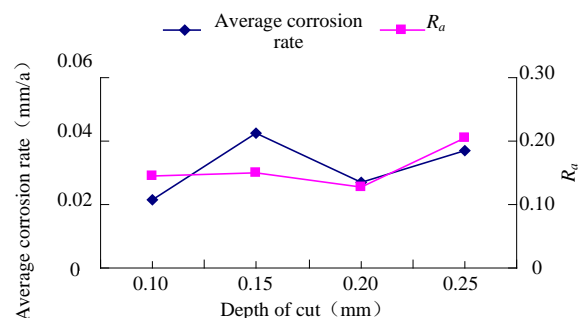


Figure 11. Influence of depth of cut on surface roughness and corrosion rate.

5. Conclusion

In order to be more intuitive to characterize the surface morphology of different milling parameters and evaluate the degree of corrosion, this paper defines Motif area ratio parameter. It is defined as the ratio of the surface area that can meet the threshold condition to the machined surface.

Through the experiment found that average corrosion rate varies with the change of surface roughness. The larger the surface roughness, the faster the average corrosion rate. Conversely the smaller the surface roughness, the slower the average corrosion rate. Based on the theoretical analysis,

machined surface topography contains a large amount of information, including the surface roughness. If the workpiece surface topography is poorer, the workpiece surface roughness value is relatively large, therefore, the workpiece surface is easy to store large amounts of corrosive medium, combined with the increased surface defects on the workpiece, all this reasons eventually result in that average corrosion rate increased. Therefore, there is a correlation of average corrosion rate and surface roughness.

6. Acknowledgments

This work was supported by Shandong Natural Science Foundation of China (No. ZR2017LEE015), Key R & D projects (civil military integration) of Shandong, China.

7. References

- [1] Ezugwu E O, Bonney J and Yamane Y 2003 *J. Materials Proc. Tech.* 134 233
- [2] Herbert C R J, Axinte D A, Hardy M C and Brown P D 2011 *Procedia Engineering* 19 138
- [3] Liu Y, Ning Y, Yao Z, Li H and Miao X 2016 *J. of Alloys and Compounds* 675 73
- [4] Liu Y, Yao Z, Ning Y, Li H and Nan Y 2016 *J. of Alloys and Compounds* 691 554
- [5] Zhang M, Li F, Yuan Z, Li J and Wang S 2013 *Materials & Design* 49 705
- [6] Zhang M J, Li F G, Wang S Y and Liu C Y 2011 *Materials Science and Eng.: A* 528 4030
- [7] Zhong B, Wang Y, Wei D, Zhang K and Wang J 2018 *Int. J. of Fatigue* 109 26
- [8] Devillez A, Schneider F, Dominiak S, Dudzinski D and Larrouquere D 2007 *Wear* 262 931
- [9] Hao Z P, Fan Y H, Lin J Q and Yu Z X 2015 *Int. J. Adv. Manuf. Tech.* 78 1329
- [10] Hardy M C, Herbert C R J, Kwong J, Li W, Axinte D A, Sharman A R C Encinas-Oropesa A and Withers P J 2014 *Procedia CIRP* 13 411
- [11] Ginting A and Nouari M 2009 *Int. J Machine Tool & Manufacturing* 49 325
- [12] Liu J, Sun J and Chen W 2017 *Int. J. Adv. Manuf. Tech.* 92 1
- [13] Varote N and Joshi SS 2017 *J. Materials Eng. and Perf.* 26 4391
- [14] Arrazola P J, Kortabarria A and Madariaga A 2014 *Simu. Mod. Prac. and Theo.* 41 87
- [15] Özel T and Ulutan D 2012 *CIRP Annals* 61 547
- [16] Madariaga A, Arrazola PJ, Esnaola JA, Ruiz-Hervias J and Muñoz P 2014 *Proc. CIRP* 13 175